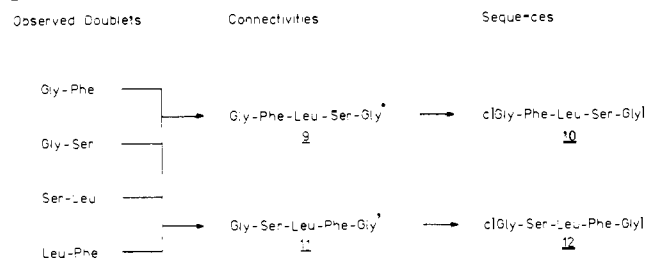


Scheme IV



decarbonylated fragment ion undergoes a facile unimolecular decomposition to give m/z 202 (100%), which arises from the loss of 119 daltons (C_8H_9N). This process has already been referred to in eq 3 and is indicative of the presence of a peptide $-^+NH=CH-CH_2Ph$ unit in an immonium ion. Consequently, the tetrapeptide immonium ion m/z 321 generated via loss of Leu and CO from the protonated pentapeptide must have the sequence Ser-Gly-Gly- $-^+NH=CH-CH_2Ph$ and *not* Phe-Gly-Gly- $-^+NH=CH-CH_2OH$. This result, in turn, is taken to rule out sequence

11 and leaves **9** as the only remaining option. Head-to-tail connection yields **10** as the correct sequence of the cyclic pentapeptide. This conclusion is in agreement with the independent sequence assignment of this peptide (based on synthesis and NMR studies) by Kessler et al.^{20,21} c[Gly-Phe-Leu-Ser-Gly] (**10**) is an important enkephaline analogue whose conformational properties and biological activity have been reported elsewhere.²¹

By applying the strategy outlined in this paper, various cyclic tetra- to hexapeptides (including somatostatin analogues)¹⁹ have been successfully sequenced. The amount of sample used in all cases was in the 5–100 nmol range.

Acknowledgment. The support of the Deutsche Forschungsgemeinschaft (Sonderforschungsbereich SFB 9), the Fonds der Chemischen Industrie, and the Midwest Center for Mass Spectrometry, a National Science Foundation regional instrumentation facility (Grant No. CHE-8211164), is appreciated. We are particularly grateful to Prof. Horst Kessler, Universität Frankfurt, and his research group for the generous supply of numerous cyclopeptides, and their helpful discussions during a stay of K.E. in Frankfurt, October 1984.

Prediction of Silicon-29 Nuclear Magnetic Resonance Chemical Shifts Using a Group Electronegativity Approach: Applications to Silicate and Aluminosilicate Structures

Nathan Janes and Eric Oldfield*†

Contribution from the School of Chemical Sciences, University of Illinois at Urbana-Champaign, Urbana, Illinois 61801. Received December 17, 1984

Abstract: Linear relations between group electronegativity (EN) sums of ligands bonded to tetravalent silicon and silicon-29 nuclear magnetic resonance (NMR) chemical shift (δ_{Si}) are shown to exist for both type P silicon (all ligands have lone-pair electrons available for (d-p) π -bonding, e.g., in $(MeO)_4Si$) and type S silicon (all ligands have only σ -bonding electrons available, e.g., in $(CH_3)_4Si$). For type P silicon having group electronegativity sums greater than 11, a range encompassing all minerals, we have used previously reported EN and δ_{Si} values (for aryl-, halo-, and alkoxysilanes) to describe the observed silicon-29 NMR chemical shift as $\delta(Si,P) = -24.336 \sum EN(P) + 279.27$. We then apply this correlation to a wide range of silicates and aluminosilicates (containing insular (Q^0) to framework (Q^4) Si sites) to predict silicon-29 NMR chemical shifts by means of a group fragment electronegativity sum approach, in which all fragments (e.g., OAl, OLi, OCa) attached to Si are assigned, on the basis of experiments on a series of model silicates and the above equation, a characteristic group (or fragment) electronegativity value. OSi group electronegativities are scaled linearly with bridging bond angle. As an example of the use of the method, the electronegativity sum value for the cyclosilicate (Q_2) beryl ($Al_2Be_3(SiO_3)_6$) is derived as $EN(OBe) + EN(OAl) + 2(EN(OSi)) (168.2^\circ) = 15.67$, which predicts a silicon-29 chemical shift of -102.1 ppm (from Me_4Si), that compares favorably with the value from experiment, -102.6 ppm. On the basis of a total of 99 sites in 51 different compounds, the mean absolute deviation between theory and experiment is 1.96 ppm (correlation coefficient = 0.979). When all types of silicon are considered (Q^0 – Q^4), this empirical approach is the most accurate method of predicting silicon-29 chemical shifts found to date.

Since 1980, there has been very considerable interest in using solid-state silicon-29 nuclear magnetic resonance (NMR) spectroscopy, with "magic-angle" sample-spinning (MASS), to investigate the structures of a wide variety of silicate and aluminosilicate materials of interest in chemistry and geochemistry.^{1–5} In order to interpret the silicon-29 shifts observed in structural terms, various correlations based on bond length,⁶ bridging bond angle,^{7,8} bond strength,^{9,10} mean TOT distance,¹¹ and σ -orbital hybridization¹² have been presented, together with a recent calculation of the paramagnetic shift term (σ_p) based on band-gap and refractive index dispersion data.¹³

To date, when *all* silicate phases are examined, the best correlation between experiment and prediction is by use of the

†E.O. was a U.S.P.H.S. Research Career Development Awardee, 1979–1984 (Grant CA-00595).

- (1) E. Lippmaa, M. Magi, A. Samoson, G. Engelhardt, and A.-R. Grimmer, *J. Am. Chem. Soc.*, **102**, 4889 (1980).
- (2) E. Lippmaa, M. Magi, A. Samoson, M. Tarmak, and G. Engelhardt, *J. Am. Chem. Soc.*, **103**, 4992 (1981).
- (3) C. A. Fyfe, J. M. Thomas, J. Klinowski, and G. C. Gobbi, *Angew. Chem., Int. Ed. Engl.*, **22**, 259 (1983).
- (4) C. A. Fyfe, G. C. Gobbi, J. Klinowski, J. M. Thomas, and S. Ramdas, *Nature (London)*, **296**, 530 (1982).
- (5) E. Oldfield and R. J. Kirkpatrick, *Science*, **227**, 1537 (1985).
- (6) J. B. Higgins and D. E. Woessner, *EOS (Trans. Am. Geophys. Union)*, **63**, 1139 (1982). A.-R. Grimmer, R. Peter, E. Fechner, and G. Molgedey, *Chem. Phys. Lett.*, **77**, 331 (1981). A.-R. Grimmer and R. Radeaglia, *Chem. Phys. Lett.*, **106**, 262 (1984).

bond-strength-bond-energy relation of Brown and Shannon¹⁴ as used by Smith et al.,^{9,15} although better correlations are available when only restricted classes of compounds, containing solely, e.g., Q⁴(4Al) sites, are investigated.^{7,8,11,12}

In this paper, we propose an improved chemical shift correlation based on group electronegativity,¹⁶ which we believe has considerable promise for giving very accurate silicon-29 chemical shift predictions for all types of silicates and aluminosilicates. The approach is applied to a total of 99 sites in 51 minerals, with mean agreement between experimental and predicted chemical shift of 1.96 ppm and a correlation coefficient of 0.979.

Results and Discussion

It has long been known, but perhaps not generally appreciated, that silicon atoms in very different chemical environments may have very similar isotropic ²⁹Si NMR chemical shifts. For example, disilane (Si₂H₆) resonates at -104.8 ppm from tetramethylsilane (Me₄Si) while quartz (SiO₂) resonates at -107.4 ppm. This observation is perhaps best expressed by the U-shaped curve shown in Figure 1A, which relates the chemical shift to the *group electronegativity sum* of the four ligands bonded to silicon.¹⁶ Group electronegativity, as its name implies, is simply the electronegativity of a given group,¹⁷ rather than a single atom, as conventionally used.¹⁸ For example, in Si(OMe)₄, the group electronegativity involved will be that of a methoxy group (3.7), and the group electronegativity sum is simply 4 × 3.7 = 14.8.

The relation in Figure 1A exhibits considerable scatter, but there is clearly a maximum deshielding at a group electronegativity sum of about 11. This maximum very nearly coincides with the point (11.8) above which Pauling has invoked (d-p) π-bonding effects to satisfy his electroneutrality principle for silicon,¹⁹ which has recently been shown to be valid in quartz²⁰ and is in accord with our LCAO analysis of the oxygen-17 nuclear quadrupole coupling constant in silica.²¹ These results suggest the presence of (d-p) π-bonding for systems having group electronegativity sums greater than ~11, as is the case for silicates and aluminosilicates.

In order to simplify the analysis of the results of Figure 1A, we define three types of silicon:

Type S silicon: all ligands are σ-bonded only and lack the lone-pair p-hybridized orbitals necessary for further conjugation (e.g., Me₄Si, H₃SiCCl₃).

Type P silicon: all ligands are capable of σ- and π-bonding (e.g., (C₆H₅)₂SiF₂, (CH₃O)₄Si).

Type M silicon: the ligands are mixed, so silicon is coordinated to both S and P ligand types (e.g., H₂SiF₂, CH₃Si(OCH₃)₃).

In this manner we seek (1) to separate σ and π-bonding effects and (2) to account for the different implications of the group

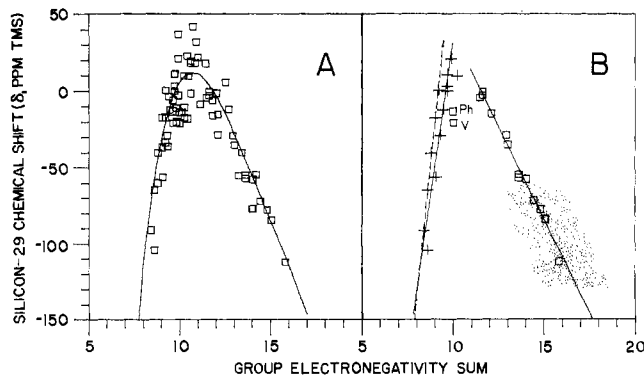


Figure 1. Graphs relating the observed silicon-29 NMR chemical shift of a given species to the electronegativity sum of the ligands bonded to silicon. (A) Type S, M, and P silicon atoms (see text for details). In order of increasing electronegativity sum, the compounds used and their shifts, group electronegativity sums, and type (δ, Me₄Si; ΣEN; type) are as follows (from ref 16 and 26): SiH₄ (-91.9, 8.4, S), Si₂H₆ (-104.8, 8.6, S), CH₃SiH₃ (-65.2, 8.6, S), (CH₃)₂SiH₂ (-40.5, 8.8, S), (C₆H₅)₃SiH₃ (-60.5, 8.8, M), (CH₃)₃SiH (-17.5, 9.0, S), C₆H₅CH₂SiH₂ (-36.9, 9.0, M), H₃SiCH₂Cl (-56.48, 9.05, S), (CH₃)₄Si (0.0, 9.2, S), C₆H₅(C₆H₅)₂SiH (-17.6, 9.2, M), (C₆H₅)₂SiH₂ (-33.9, 9.2, M), ClSiH₃ (-36.1, 9.3, M), H₃SiCCl₃ (-28.96, 9.3, S), C₆H₅Si(CH₃)₃ (-4.0, 9.4, M), CH₂Cl(CH₃)₂SiH (-12.29, 9.45, S), (C₆H₅)₂SiH (-21.1, 9.6, M), (C₆H₅)₂Si(CH₂)₂ (-6.5, 9.6, M), (C₂H₅)₂Si(CH₂)₂ (-13.7, 9.6, M), (C₆H₅)₃SiCH₂OH (-0.3, 9.7, S), (CH₃)₃SiCH₂Cl (3.1, 9.7, S), (CH₃)₃SiCH₂HCl₂ (10.5, 9.7, S), (CH₃)₂HSiCl (11.10, 9.73, M), (C₂H₅)₃SiCH₃ (-20.6, 9.8, M), (C₆H₅)₃SiCH₃ (-11.5, 9.8, M), ((CH₃)₃)₂SiCH₃ (36.5, 9.9, M), (C₆H₅)₂(CH₃)₂SiCH₂Cl (-3.3, 9.9, M), (CH₃)₃SiCCl₃ (20.73, 9.9, S), (C₂H₅)₄Si (-21.5, 10.0, P), (C₆H₅)₄Si (-13.98, 10.0, P), (C₂H₅)₂C₆H₅SiCH₂Cl (-14.0, 10.1, M), (CH₃)₂Si(CH₂)₂ (9.75, 10.2, S), H₃SiF (-17.40, 10.25, M), H₂SiCl₂ (-11.03, 10.26, M), (CH₃)₂ClSiCHCl₂ (22.6, 10.4, M), (C₆H₅)₂CH₂SiH (-18.5, 10.4, M), CH₃HSiCl₂ (9.7, 10.46, M), (C₂H₅)₃SiOH (19.3, 10.6, M), (CH₃)₂SiOCH₃ (18.0, 10.6, M), C₆H₅SiHCl₂ (-2.2, 10.6, M), (CH₃)₂SiCl₂ (41.5, 10.7, M), C₆H₅SiCH₂Cl₂ (17.9, 10.86, M), (CH₃)₃SiF (31.9, 10.9, M), CH₃Cl₂SiCH₂Cl (21.6, 11.0, M), Cl₃SiH (-9.3, 11.1, M), CH₃SiCl₃ (17.5, 11.4, M), (C₆H₅)₃SiF (-4.7, 11.45, P), C₂H₅SiCl₃ (-3.5, 11.6, P), C₆H₅SiCl₃ (-0.8, 11.6, P), Cl₃SiCHCl₂ (-6.5, 11.8, M), (C₂H₅O)₂CH₂SiH (-16.1, 11.8, M), (C₆H₅)₂Si(OCH₃)₂ (-1.5, 12.0, M), SiCl₄ (-15.5, 12.1, P), H₂SiF₂ (-28.50, 12.1, M), (CH₃)₂SiF₂ (5.3, 12.5, M), CH₃F₂SiC₆H₅ (-12.4, 12.7, M), (C₆H₅)₂SiF₂ (-29.5, 12.9, P), Cl₃SiF (-35.6, 13.0, P), (CH₃O)₃SiH (-55.6, 13.2, M), CH₃Si(OCH₃)₃ (-40.5, 13.4, M), (CH₃O)₃SiC₆H₅ (-55.25, 13.6, P), C₆H₅Si(OCH₃)₃ (-57.5, 13.6, P), HSiF₃ (-77.77, 13.95, M), Si₂F₆ (-77.5, 14.0, M), Cl₂SiF₂ (-58.5, 14.0, P), CH₃SiF₃ (-55.3, 14.2, M), C₆H₅SiF₃ (-72.5, 14.4, P), (CH₃O)₄Si (-78.5, 14.8, P), ClSiF₃ (-85.2, 15.0, P), FSi(OC₂H₅)₃ (-84.5, 15.05, P), SiF₄ (-112.5, 15.8, P). The equation for the curve is from ref 26. (B) As in part A but with only type S and type P silicon. The tetraphenyl and tetravinyl silanes are labeled Ph and V, respectively. Best linear fits are indicated by the solid lines; the dotted line is for the series Me_{4-n}SiH_{4-n}. The stippled area represents the range of chemical shifts found for minerals.

electronegativity concept for different ligand types. Since the group electronegativity is a characteristic of the ligand and all available bonding orbitals, the degree of covalent charge transfer is dependent on the number of available bonding orbitals per ligand as well as the silicon-ligand electronegativity difference.^{19,20,22} Others have shown that the effective silicon charge calculated by CNDO/2 methods is strongly correlated with chemical shift for compounds on both sides of the U-curve inflection. Correlations with either the σ or π contributions alone were less successful.^{16,23}

Using these definitions, we show in Figure 1B the data from Figure 1A for type S and type P silicon. Much of the scatter in Figure 1A is clearly due to species containing type M silicon, since a much more regular trend emerges for the S and P type silicon resonances. The stippled area in Figure 1B encompasses the chemical shift range found for silicates and aluminosilicates.

(22) L. Pauling, *Am. Miner.*, **65**, 321 (1980).

(23) A. M. Krapivin, M. Magi, V. I. Svergun, R. Z. Zaharjan, E. D. Babich, and N. V. Ushakov, *J. Organomet. Chem.*, **190**, 9 (1980).

(7) J. V. Smith and C. S. Blackwell, *Nature (London)*, **303**, 223 (1983). J. V. Smith, C. S. Blackwell, and G. L. Hovis, *Nature (London)*, **309**, 140 (1984).

(8) J. M. Thomas, J. Klinowski, S. Ramdas, B. K. Hunter, and D. T. B. Tennakoon, *Chem. Phys. Lett.*, **102**, 158 (1983).

(9) K. A. Smith, R. J. Kirkpatrick, E. Oldfield, and D. M. Henderson, *Am. Miner.*, **68**, 1206 (1983). K. A. Smith and R. J. Kirkpatrick, unpublished results.

(10) M. Magi, E. Lippmaa, A. Samoson, G. Engelhardt, and A.-R. Grimmer, *J. Phys. Chem.*, **88**, 1518 (1984).

(11) S. Ramdas and J. Klinowski, *Nature (London)*, **308**, 521 (1984). M. O'Keefe and B. G. Hyde, In "Structure and Bonding in Crystals", M. O'Keefe and A. Navrotsky, Eds., Vol. 1, Academic Press, New York, 1981, pp 227-254.

(12) G. Engelhardt and R. Radeaglia, *Chem. Phys. Lett.*, **108**, 271 (1984).

(13) J. A. Tossell, *Phys. Chem. Miner.*, **10**, 137 (1984).

(14) I. D. Brown and R. D. Shannon, *Acta Crystallogr., Sect. A*, **29**, 266 (1973).

(15) N. Janes, K. A. Smith, R. J. Kirkpatrick, D. M. Henderson, R. Oestrike, and E. Oldfield, unpublished results.

(16) C. R. Ernst, L. Spialter, G. R. Buell, and D. L. Wilhite, *J. Am. Chem. Soc.*, **96**, 5375 (1974).

(17) P. R. Wells, In "Progress in Physical Organic Chemistry", Vol. 6, Interscience Publishers, New York, 1968, pp 111-145.

(18) W. Gordy and W. J. Orville-Thomas, *J. Chem. Phys.*, **24**, 439 (1956).

(19) L. Pauling, "The Nature of the Chemical Bond", Cornell University Press, Ithaca, New York, 1960.

(20) R. F. Stewart, M. A. Whitehead, and G. Donnay, *Am. Miner.*, **65**, 324 (1980).

(21) N. Janes and E. Oldfield, unpublished results.

Table I. Chemical Shifts, Group Electronegativity Sums, and Group Electronegativities for a Series of Silicates

group	compound	mean SiOSi angle (deg)	chemical shift (δ) ^a	ΣEN ^b	group electronegativity
OLi	Li ₂ SiO ₃ (lithium metasilicate)	124 ^c	-74.5 ^d	14.5370	3.4385
ONa	Na ₂ SiO ₃ (sodium metasilicate)	133.7 ^e	-78.0 ^f	14.6808	3.4395
OMg	Mg ₂ SiO ₄ (forsterite)		-61.9 ^f	14.0192	3.5048
OH	NaH ₃ SiO ₄		-66.4 ^d	14.2042	3.5882
OBa	Ba ₂ SiO ₄		-70.3 ^f	14.3644	3.5911
OCa	α,β,γ-Ca ₂ SiO ₄ (av)		-71.7 ^d	14.4233	3.6058
OBe	Be ₂ SiO ₄		-74.2 ^d	14.5247	3.6312
OGa	zeolite Q ⁴ (4Ga)		-77.5 ^g	14.6603	3.6651
OAl	zeolite Q ⁴ (4Al)		-84.2 ^h	14.9356	3.7339
OSi	SiO ₂ (low quartz)	143.6 ⁱ	-107.4 ^j	15.8888	3.9722 ^k
OSi	SiO ₂ (low cristobalite)	146.8 ^l	-109.9 ^j	15.9916	3.9979 ^k
OSi	SiO ₂ (coesite T ₁)	180.0 ^{m,n}	-113.9 ^o	16.1559 ⁿ	4.2393 ^k

^aIn ppm from an external sample of tetramethylsilane. ^bGroup electronegativity sum obtained by using eq 1 in the text. ^cFrom ref 41. ^dFrom ref 10. ^eFrom ref 42. ^fFrom ref 9. ^gAverage value based on all available Q⁴(4Ga) sites in gallosilicates compiled in ref 43. ^hAverage value based on all available Q⁴(4Al) sites in zeolites compiled in ref 2. ⁱFrom ref 44. ^jFrom ref 1. ^kValues employed for eq 3, see text. ^lFrom ref 45. ^mFrom ref 46. ⁿOne linear SiOSi bond; average bridging angle for remaining three ligands is 143.7° and assumed to be described by the quartz value. ^oFrom ref 7.

For the type P silicon resonances an excellent correlation (0.992) is obtained between the silicon-29 chemical shift and the group electronegativity sum, but only if the points for tetraphenyl- and tetravinylsilane are ignored (otherwise the correlation coefficient drops to 0.912). We believe it is reasonable to ignore these two points, despite evidence for (d-p) π-bonding effects (or alternatively (σ*-p) hyperconjugation²⁴) presented for the vinylsilanes,²⁵ since in Pauling's scheme these effects are considered rather small, because the low electronegativity sum (10.0) implies that the electroneutrality principle holds even without invoking π back-bonding. Thus, in our classification we consider only type P sites where the group electronegativity sum (ΣEN) is greater than 11.

For type P silicon sites, the observed chemical shift may thus be expressed as

$$\delta_{\text{Si}}(\text{P}) = -24.336 \Sigma \text{EN}(\text{P}) + 279.27 \quad (1)$$

For type S silicon sites, we obtain a more modest correlation

$$\delta_{\text{Si}}(\text{S}) = 81.871 \Sigma \text{EN}(\text{S}) - 784.59 \quad (2)$$

(correlation coefficient = 0.891). The correlation obtained for the methylsilanes (Me_{4-n}SiH_n), however, is much higher (0.997, dotted line in Figure 1B), which may indicate long-range effects on the ²⁹Si shifts due to lone pairs on atoms not directly bonded to silicon.²⁶

The results presented above thus suggest that group electronegativities may be used to predict silicon-29 chemical shifts of both type S and type P silicon atoms, and the excellent correlation observed with type P sites forms the basis for our use of the method to predict ²⁹Si shifts in minerals (or glasses, ceramics, zeolite catalysts, etc.).

In order to use the method, the first step is to establish a series of group electronegativities for the various oxy-metal fragments, such as OLi, OSi, OAl, etc., to which silicon is bonded in the silicate or aluminosilicate of interest. Group electronegativities may be calculated on a semiempirical basis, as most recently described by Mullay;²⁷ however, in this publication we derive them experimentally, thereby empirically accounting for complex crystal structure effects. This is readily achieved by use of eq 1 (Figure 1B) and the series of model compounds listed in Table I. The group electronegativities of the oxy-alkaline earth metal fragments are obtained from the experimental chemical shifts of the M₂SiO₄ nesosilicates. The OAl and OGa values were derived from the average shift of a number of Q⁴(4T) zeolites. Similar suitable model compounds were unavailable for certain fragments (e.g., ONa, OH), so their group electronegativities were obtained from

the ΣENs of more complex compounds, by difference. For example, the ONa group electronegativity was derived from the ΣEN of sodium metasilicate (Na₂SiO₃), and for consistency, the OLi value was derived from lithium metasilicate (Li₂SiO₃). As a result, these values may be less accurate.

The main drawback of the method as presented thus far is of course one of oversimplification—the choice of one group (fragment) electronegativity to describe all bonding situations. Minerals have a very rich structural complexity with respect to bond lengths, bridging-oxygen bond angles, and degree of both oxygen and metal coordination. The group electronegativities discussed above are blind to these more subtle structural features and treat each group identically regardless of bonding situation. For instance, we have derived empirically a group electronegativity for OCa from the average shift of the α-, β-, and γ-Ca₂SiO₄ polymorphs. Within the Q⁰ calcium silicates the range of silicon-29 chemical shifts extends about 6 ppm, thus the model is accurate to only about 3 ppm for the average empirical OCa group electronegativity.

Since the range of silicon-29 chemical shifts for the Q⁴(4Si) sites extends some 25 ppm, the OSi group electronegativity is expected to have an even wider range of possible values. This may be attributed to variations in the bridging-oxygen bond angles^{7,8,10,12} which are believed to influence the oxygen orbital electronegativities.²⁸ In order to account for this structural effect, we have derived the OSi group electronegativity as a function of bridging bond angle, using the compounds low quartz and low cristobalite and a value for the linear OSi group from the Si(1) site of coesite (assuming one linear OSi and three quartz-like OSi bonds). Albeit for only three minerals, a linear correlation of 0.99997 is observed between the group electronegativity and bridging bond angle as follows

$$\text{EN}(\text{OSi}) = (\angle \text{SiOSi} / 136.79) + 2.9235 \quad (3)$$

This relation permits use of a sliding scale of OSi group electronegativities and, although approximate, allows partial compensation for the variation of group electronegativity with bridging bond angle.

The empirically derived electronegativity values are broadly as expected. The group IA and group IIA oxymetal values are less than that of methoxy, while the linear OSi value is greater than that of fluorine, as expected for sp-hybridized oxygen.²⁸ The apparent OCa and OBa electronegativities are somewhat enhanced, perhaps due to crystallographic effects for these larger cations.

The group electronegativity sum of a given Qⁿ silicon site is determined as follows:

$$\Sigma \text{EN}(\text{Q}^n) = \Sigma \text{EN}_f + (4 - n) \Sigma (\text{EN}_{\text{nt}z_{\text{nt}}} / \Sigma z_{\text{nt}}) \quad (4)$$

n represents the total number of framework (groups IIIB, IVB,

(24) C. G. Pitt, *J. Organomet. Chem.*, **61**, 49 (1973).
 (25) L. Delmule and G. P. Van der Kelen, *J. Mol. Struct.*, **66**, 309 (1980).
 (26) H. Marsmann, In "NMR Basic Principles and Progress", P. Diehl, E. Fluck, and R. Kosfeld, Eds., Vol. 17, Springer-Verlag, New York, 1981.
 (27) J. Mullay, *J. Am. Chem. Soc.*, **106**, 5842 (1984).

(28) J. Hinze and H. H. Jaffe, *J. Am. Chem. Soc.*, **84**, 540 (1962).

Table II. Comparison between Observed and Predicted Silicon-29 NMR Chemical Shifts for a Series of Silicates and Aluminosilicates

compound	name	site	mean SiOSi angle (deg)	Σ EN	δ (calcd) (ppm) ^a	δ (obsd) (ppm) ^a	error (ppm) ^b
Li ₄ SiO ₄		Q ⁰		13.7540	-55.4	-64.9 ^c	-9.5
CaMgSiO ₄	monticellite	Q ⁰		14.2212	-66.8	-66.3 ^d	+0.5
Na ₆ Si ₂ O ₇		Q ¹	136.4 ^e	14.2391	-67.2	-68.4 ^c	-1.2
Ca ₂ Al ₂ SiO ₇	gehlenite	Q ¹ (1Al)		14.7160	-78.9	-72.5 ^d	+6.4
CaNaHSiO ₄		Q ⁰		14.2393	-67.3	-73.5 ^c	-6.2
Ca ₂ MgSi ₂ O ₇	akermanite	Q ¹	139.4 ^f	14.6590	-77.5	-73.7 ^d	+3.8
Ca ₃ Si ₂ O ₇	rankinite	Q ¹	136.2 ^g	14.7366	-79.4	-74.5 ^c	+4.9
		Q ¹	136.2 ^g	14.7366	-79.4	-76.0 ^c	+3.4
Al ₂ SiO ₅	andalusite	Q ⁰		14.9356	-84.2	-79.9 ^d	+4.3
BaSiO ₃	barium metasilicate	Q ²	128.2 ^d	14.9036	-83.4	-80.3 ^d	+3.1
Al ₂ SiO ₅	kyanite	Q ⁰ (T ₁ ,T ₂)		14.9356	-84.2	-83.2 ^d	+1.0
Ca ₃ Al ₂ (SiO ₄) ₃	grossular garnet	Q ⁰		14.6794	-78.0	-83.4 ^d	-5.4
α -Ca ₃ [Si ₃ O ₉]	psuedowollastonite	Q ² (T ₁ to T ₆)	135 ^h	15.0324	-86.6	-83.5 ^c	+3.1
Mg ₂ Si ₂ O ₆	clinoenstatite	Q ² (TA)	133.3 ⁱ	14.8056	-81.0	-84.2 ^{d,j}	-3.2
		Q ² (TB)	127.5 ⁱ	14.7208	-79.0	-81.8 ^{d,j}	-2.8
CaMgSi ₂ O ₆	diopside	Q ²	135.93 ^k	14.9450	-84.4	-84.7 ^d	-0.3
β -Ca ₃ [Si ₃ O ₉]	parawollastonite	Q ² (T ₁ ,T ₂)	145.5 ⁱ	15.1859	-90.3	-84.5 ^c	+5.8
		Q ² (T ₃)	140.3 ⁱ	15.1099	-88.4	-84.5 ^c	+3.9
Ca ₂ NaHSi ₃ O ₉	pectolite	Q ² (T ₁)	141.4 ⁱ	15.0647	-87.3	-86.3 ^m	+1.0
		Q ² (T ₂)	142.1 ⁱ	15.0749	-87.6	-86.3 ^m	+1.3
		Q ³ (T ₃)	135.7 ⁱ	14.9814	-85.3	-86.3 ^m	-1.0
Al ₂ SiO ₅	sillimanite	Q ³ (3Al)		14.9356	-84.2	-86.9 ^d	-2.7
β -Ca ₃ [Si ₃ O ₉]	wollastonite	Q ² (T ₁)	145.40 ⁱ	15.1845	-90.3	-89.2 ^d	+1.1
		Q ² (T ₂)	145.15 ⁱ	15.1808	-90.2	-89.2 ^d	+1.0
		Q ³ (T ₃)	140.05 ⁱ	15.1063	-88.4	-89.2 ^d	-0.8
LiAlSi ₂ O ₆	spodumene	Q ²	139.0 ^k	15.1994	-90.6	-91.6 ^c	-1.0
NaAlSi ₂ O ₆	jadeite	Q ²	139.1 ^k	15.2104	-90.7	-91.8 ^c	-1.1
Ca ₂ Mg ₅ Si ₈ O ₂₂ (OH) ₂	tremolite	Q ³ (T ₁)	138.07 ⁿ	15.3322	-93.8	-92.2 ^c	+1.6
		Q ² (T ₂)	137.45 ⁿ	14.9240	-83.9	-87.8 ^c	-3.9
Li ₂ Si ₂ O ₅	lithium disilicate	Q ³	137.3 ^o	15.2209	-91.1	-92.7 ^d	-1.6
α -Na ₂ Si ₂ O ₅	α -sodium disilicate	Q ³	145.97 ^d	15.4113	-95.8	-94.6 ^d	+1.2
NaAlSi ₃ O ₈	albite	Q ⁴ (2Al)T ₂ m	145.85 ^p	15.4473	-96.6	-92.3 ^p	+4.3
		Q ⁴ (1Al)T ₂ O	139.13 ^p	15.5558	-99.3	-96.9 ^p	+2.4
		Q ⁴ (1Al)T ₁ m	149.37 ^p	15.7803	-104.8	-104.3 ^p	+0.5
KAlSi ₃ O ₈	microcline	Q ⁴ (2Al)T ₂ m	147.21 ^p	15.4672	-97.1	-95.4 ^p	+1.7
		Q ⁴ (1Al)T ₂ O	137.45 ^p	15.5188	-98.4	-97.8 ^p	+0.6
		Q ⁴ (1Al)T ₁ m	143.27 ^p	15.6466	-101.5	-100.4 ^p	+1.1
Al ₂ Be ₃ (SiO ₃) ₆	beryl	Q ²	168.24 ^q	15.6719	-102.1	-102.6 ^c	-0.5
LiAlSi ₄ O ₁₀	petalite	Q ⁴ (1Al)T ₁	159.78 ^r	16.0086	-110.3	-110.9 ^d	-0.6
		Q ⁴ (1Al)T ₂	154.11 ^r	15.8843	-107.3	-109.5 ^d	-2.2
Na ₄ Ca ₈ [(AlO ₂) ₂₀ (SiO ₂) ₂₀] \cdot 24H ₂ O	thomsonite (1.0) ^s	Q ⁴ (4Al)		14.9356	-84.2	-83.5 ⁱ	+0.7
Na ₆ [(AlO ₂) ₆ (SiO ₂) ₆] \cdot 7.5H ₂ O	hydrated sodalite (1.0) ^s	Q ⁴ (4Al)		14.9356	-84.2	-83.5 ⁱ	+0.7
Na ₈ [(AlO ₂) ₆ (SiO ₂) ₆] \cdot Cl ₂ \cdot xH ₂ O	sodalite (1.0) ^s	Q ⁴ (4Al)		14.9356	-84.2	-84.8 ⁱ	-0.6
Li ₁₂ [(AlO ₂) ₁₂ (SiO ₂) ₁₂] \cdot 27H ₂ O	Linde Li-A zeolite (1.0) ^s	Q ⁴ (4Al)		14.9356	-84.2	-85.0 ^u	-0.8
Na ₆ [(AlO ₂) ₆ (SiO ₂) ₆] \cdot xH ₂ O	cancrinite (1.0) ^s	Q ⁴ (4Al)		14.9356	-84.2	-87.2 ^u	-3.0
Na ₅₅ [(AlO ₂) ₅₅ (SiO ₂) ₁₃₇] \cdot 250H ₂ O	Linde Na-Y zeolites (2.5) ^s	Q ⁴ (4Al)		14.9356	-84.2	-83.8 ⁱ	+0.4
		Q ⁴ (3Al)	144.8 ^u	15.1838	-90.2	-89.2 ⁱ	+1.0
		Q ⁴ (2Al)	144.8 ^u	15.4319	-96.3	-94.5 ⁱ	+1.8
		Q ⁴ (1Al)	144.8 ^u	15.6801	-102.3	-100.0 ⁱ	+2.3
		Q ⁴ (0Al)	144.8 ^u	15.9282	-108.4	-105.5 ⁱ	+2.9
Na ₁₂ [(AlO ₂) ₁₂ (SiO ₂) ₁₂] \cdot 27H ₂ O	Linde Na-A zeolite (1.0) ^s	Q ⁴ (4Al)		14.9356	-84.2	-88.9 ^u	-4.7
Na ₈₈ [(AlO ₂) ₈₈ (SiO ₂) ₁₀₄] \cdot 264H ₂ O	Linde Na-X zeolite (1.18) ^s	Q ⁴ (4Al)		14.9356	-84.2	-84.6 ⁱ	-0.4
		Q ⁴ (3Al)	139.2 ^u	15.1428	-89.2	-89.0 ⁱ	+0.2
		Q ⁴ (2Al)	139.2 ^u	15.3500	-94.3	-94.2 ⁱ	+0.1
		Q ⁴ (1Al)	139.2 ^u	15.5573	-99.3	-98.8 ⁱ	+0.5
		Q ⁴ (0Al)	139.2 ^u	15.7645	-104.4	-103.1 ⁱ	+1.3
Na ₇ ((CH ₃) ₄ N)[(AlO ₂) ₈ (SiO ₂) ₉] \cdot xH ₂ O	ZK-4 zeolite (1.14) ^s	Q ⁴ (4Al)		14.9356	-84.2	-89.1 ^u	-4.9
		Q ⁴ (3Al)	148.0 ^{u,v}	15.2072	-90.8	-93.9 ^u	-3.1
		Q ⁴ (2Al)	148.0 ^{u,v}	15.4787	-97.4	-99.5 ^u	-2.1
		Q ⁴ (1Al)	148.0 ^{u,v}	15.7503	-104.0	-106.1 ^u	-2.1
Ca ₈ [(AlO ₂) ₁₆ (SiO ₂) ₂₄] \cdot 24H ₂ O	scolecite (1.5) ^s	Q ⁴ (3Al)	138.3 ^u	15.1362	-89.1	-86.3 ^u	+2.8
		Q ⁴ (3Al)	139.3 ^u	15.1435	-89.3	-89.1 ^u	+0.2
		Q ⁴ (2Al)	147.4 ^u	15.4700	-97.2	-95.8 ^u	+1.4
Na ₁₆ [(AlO ₂) ₁₆ (SiO ₂) ₂₄] \cdot 16H ₂ O	natrolite (1.5) ^s	Q ⁴ (3Al)	137.2 ^u	15.1282	-88.9	-87.7 ^u	+1.2
		Q ⁴ (2Al)	142.4 ^u	15.3968	-95.4	-95.4 ^u	0.0
Na ₈ [(AlO ₂) ₈ (SiO ₂) ₁₆] \cdot 24H ₂ O	gmelinite (2.0) ^s	Q ⁴ (3Al)	143.3 ^u	15.1728	-90.0	-92.0 ⁱ	-2.0
		Q ⁴ (2Al)	143.3 ^u	15.4100	-95.7	-97.2 ⁱ	-1.5
		Q ⁴ (1Al)	143.3 ^u	15.6472	-101.5	-102.5 ⁱ	-1.0
Ca ₂ [(AlO ₂) ₄ (SiO ₂) ₈] \cdot 13H ₂ O	chabazite (2.0) ^s	Q ⁴ (3Al)	145.4 ^u	15.1881	-90.3	-94.0 ⁱ	-3.7
		Q ⁴ (2Al)	145.4 ^u	15.4407	-96.5	-99.4 ⁱ	-2.9
		Q ⁴ (1Al)	145.4 ^u	15.6932	-102.6	-104.8 ⁱ	-2.2
		Q ⁴ (0Al)	145.4 ^u	15.9458	-108.8	-110.0 ⁱ	-1.2
Na ₁₆ [(AlO ₂) ₁₆ (SiO ₂) ₃₂] \cdot 16H ₂ O	analcime (2.0) ^s	Q ⁴ (3Al)	144.3 ^u	15.1801	-90.1	-92.0 ⁱ	-1.9
		Q ⁴ (2Al)	144.3 ^u	15.4246	-96.1	-96.3 ⁱ	-0.2
		Q ⁴ (1Al)	144.3 ^u	15.6691	-102.0	-101.3 ⁱ	+0.7
		Q ⁴ (0Al)	144.3 ^u	15.9136	-108.0	-108.0 ⁱ	0.0

Table II (Continued)

compound	name	site	mean SiOSi angle (deg)	ΣEN	δ(calcd) (ppm) ^a	δ(obsd) (ppm) ^a	error (ppm) ^b
Ca ₄ [(AlO ₂) ₈ (SiO ₂) ₁₆]·16H ₂ O	laumontite (2.0) ^f	Q ⁴ (2Al)	138.0 ^u	15.3325	-93.9	-92.4 ^u	+1.5
Na ₂ [(GaO ₂) _{1.9} (AlO ₂) _{0.1} (SiO ₂) _{2.28}]·xH ₂ O	Na-GaX zeolite (1.14) ^f	Q ⁴ (4Ga)		14.6603	-77.5	-77.7 ^x	-0.2
		Q ⁴ (3Ga)	139.2 ^w	14.9364	-84.2	-84.2 ^x	0.0
		Q ⁴ (2Ga)	139.2 ^w	15.2124	-90.9	-90.3 ^x	+0.6
		Q ⁴ (1Ga)	139.2 ^w	15.4884	-97.7	-96.4 ^x	+1.3
		Q ⁴ (0Ga)	139.2 ^w	15.7645	-104.4	-102.8 ^x	+1.6
Na ₂ [(GaO ₂) _{1.96} (AlO ₂) _{0.04} (SiO ₂) _{4.33}]·xH ₂ O	Na-GaY zeolite (2.15) ^f	Q ⁴ (4Ga)		14.6603	-77.5	-78.3 ^x	-0.5
		Q ⁴ (3Ga)	144.8 ^w	14.9774	-85.2	-84.6 ^x	+0.6
		Q ⁴ (2Ga)	144.8 ^w	15.2943	-92.9	-91.4 ^x	+1.5
		Q ⁴ (1Ga)	144.8 ^w	15.6113	-100.6	-98.2 ^x	+2.4
		Q ⁴ (0Ga)	144.8 ^w	15.9282	-108.4	-105.8 ^x	+2.6
SiO ₂	silicalite	Q ⁴ (0Al)	150.7 ^u	16.1008	-112.6	-109.2 ^u	+3.4
		Q ⁴ (0Al)	160.6 ^u	16.3902	-119.6	-116.3 ^u	+3.3
((CH ₃) ₄ N) _{2.1} Na _{0.76} [(AlO ₂) ₂ (SiO ₂) ₁₀]·0.9H ₂ O ^v SiO ₂ ^z	TMA-sodalite (6.0) ^f ω-mazzite ^z	Q ⁴ (0Al)	157.8 ^u	16.3084	-117.6	-116.2 ^u	+1.4
		Q ⁴ (0Al)	140.8 ^u	15.8113	-105.5	-106.0 ^u	-0.5
		Q ⁴ (0Al)	151.9 ^u	16.1358	-113.4	-114.4 ^u	-1.0
SiO ₂ ^z	offretite ^z	Q ⁴ (0Al)	142.5 ^u	15.8610	-106.7	-109.7 ^u	-3.0
		Q ⁴ (0Al)	151.3 ^u	16.1183	-113.0	-115.2 ^u	-2.2
SiO ₂ ^z	mordenite ^z	Q ⁴ (0Al)	150.4 ^u	16.0920	-112.3	-112.2 ^u	+0.1
		Q ⁴ (0Al)	152.3 ^u	16.1475	-113.7	-113.1 ^u	+0.6
		Q ⁴ (0Al)	156.0 ^u	16.2557	-116.3	-115.0 ^u	+1.3
SiO ₂ [Al ₁₃ (OH,F) ₁₆ F ₂]Si ₅ O ₂₀ Cl	coesite zunyite	Q ⁴ (0Al)T ₂	143.4 ^{aa}	15.8882	-107.4	-108.1 ^{bb}	-0.7
		Q ⁴	180.0 ^{cc}	16.9575	-133.4	-128.5 ^{dd}	-4.9

^a In ppm from Me₄Si, more negative values correspond to high field, low frequency, more shielded or diamagnetic shifts. ^b Error is δ(experiment) - δ(calcd). ^c From ref 10. ^d From compilation in ref 9. ^e From ref 47; assumed isostructural with the lithium form. ^f From ref 48. ^g From ref 49. ^h From ref 50. ⁱ From ref 51. ^j Tentative assignment. ^k From ref 52. ^l From ref 53. ^m From ref 1. ⁿ From ref 54. ^o From ref 55. ^p From ref 7. ^q From ref 56. ^r From ref 27. ^s Si/(Al + Ga) ratio. ^t From ref 2. ^u From compilation given in ref 11. ^v SiOT angle assumed invariant with Si/Al ratio. ^w SiOT angle assumed invariant with gallium substitution. ^x From ref 43. ^y From ref 57. ^z [(CH₃)₄N + Na]/Al > 1.0. ^{aa} Dealuminated zeolites. ^{bb} From ref 12. ^{cc} From ref 31. ^{dd} From ref 32.

VB) tetrahedra coordinated to a given silicon tetrahedron, as opposed to the narrower definition used elsewhere^{1,10} that includes only linked silicate tetrahedra. EN_f and EN_{nf} represent the group electronegativity values listed in Table I for framework and nonframework ligands, respectively, and z_{nf} is the formal charge of a nonframework cation.

These empirically derived group electronegativities provide the basis for our prediction of the chemical shifts of a wide range of minerals. To illustrate the use of the method, we predict the silicon-29 chemical shift of the (Q²) cyclosilicate beryl, Al₂Be₃(SiO₃)₆. To do this, we simply add the group electronegativities of the four groups bonded to silicon as follows:

$$\Sigma EN = 2EN[OSi(168.2^\circ)] + 2\{2EN[OAl(\frac{2}{12})] + 3EN[OBe(\frac{3}{12})]\} = 15.6719$$

The resultant group electronegativity sum of 15.6719 for beryl corresponds to a chemical shift (using the correlation from the solution data in eq 1) of -102.1 ppm (from Me₄Si) which compares very favorably with the experimental value, -102.6 ppm.

In Figure 2, we illustrate the correlation found between the experimental chemical shifts and those predicted by using the group electronegativities tabulated in Table II, for 51 different silicates and aluminosilicates (containing a total of 99 different sites). A high correlation is observed (correlation coefficient = 0.979), corresponding to a mean absolute deviation between prediction and experiment of 1.96 ppm, which we believe indicates considerable potential for the approach in predicting ²⁹Si chemical shifts in such systems.

In zeolites, we have obtained the OSi group electronegativity by employing the mean Si-O-T bridging angle, as reported previously for other correlations.^{7,11} In structures where the identity of the aluminum and silicon sites are known, such as albite, no such approximation need be made.

By neglecting structural effects for all group electronegativities except OSi, we have developed a predictive model of good accuracy that is extremely simple to use and empirically consistent without resort to fitted parameters. However, we believe that considerable potential exists for further improvements by taking into account varying structural effects for the other groups. In general, we expect that errors due to structural effects will be magnified for compounds with low degrees of polymerization where little or no

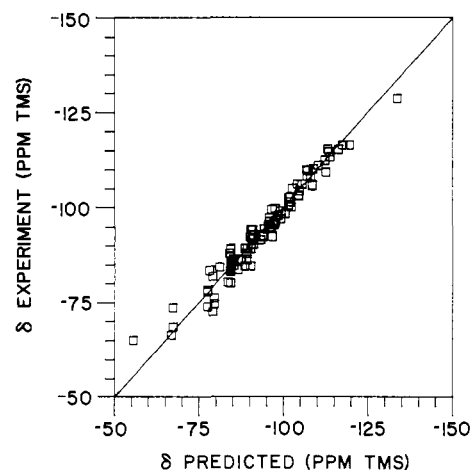


Figure 2. Graph showing correlation between experimentally determined silicon-29 MASS NMR chemical shift (in ppm from external Me₄Si) and chemical shift predicted on the basis of the group electronegativity sum (Tables I and II, see text for details). Correlation coefficient = 0.979. Solid line represents δ(experiment) = δ(predicted). The mean absolute deviation between experiment and prediction is 1.96 ppm.

attempt is made to modify the group electronegativity. As a result the mean absolute errors decrease with increasing degree of polymerization (Q⁰, |Δδ| = 4.48, n = 6; Q¹, |Δδ| = 3.94, n = 5; Q², |Δδ| = 2.21, n = 15; Q³, |Δδ| = 2.12, n = 6; Q⁴, |Δδ| = 1.57, n = 67). For example, in Li₄SiO₄ the error is 9.5 ppm (Table II), due, presumably, to use of a somewhat uncertain electronegativity value for OLi (based on Li₂SiO₃). It is our belief that a sliding scale of group electronegativities, based, for example, on the Brown and Shannon bond strength-bond length type relations,¹⁴ may be formulated to account, at least in part, for these more subtle structural effects, since recent results from our group⁹ have demonstrated a correlation between cation-oxygen bond strength sums and silicon-29 chemical shifts which shows increased shielding for overbonded (or more electronegative) oxygen. Additional corrections to the group electronegativity will also arise from changes in silicon and OAl oxygen hybridization, which influence the respective orbital electronegativities.²⁸

The inclusion of structural effects in the OSi group electronegativities facilitates interpretation of the otherwise anomalously shielded Q^2 chemical shift of beryl, (predicted -102.1 , observed -102.6), $Q^4(1A)$ shifts of petalite—which contains a linear SiOSi bond²⁹—(predicted -110.3 , -107.3 ; observed -110.9 , -109.5), as well as the central Q^4 silicon chemical shift of the Si_5O_{16} anion in zunyite ($[Al_{13}(OH,F)_{16}F_2]Si_5O_{20}Cl$), which contains four linear SiOSi bonds.^{30,31} Using the derived group electronegativity of 4.2392 (Table I), we are able to predict a chemical shift for the idealized framework structure with four 180° bridging angles of -133.4 ppm, near the Q^4 zunyite resonance of -128.5 ppm.³²

Finally, implicit within our model is the assumption that ligands influence the chemical shift in an additive manner. The high correlations observed for type P silicon ($\sum EN > 11$) in Figures 1B and 2 provide strong evidence for such additivity, which we believe has relevance not only for minerals but also for a wide range of other type P silicon compounds, and perhaps for other nuclei as well.

Comments on the (d-p) π Effect

Our intent in the preceding discussion was to present an empirical predictive model for silicon-29 chemical shifts in silicates and not necessarily to draw theoretical inferences from our empirical observations. We have, consequently, made little reference to the extensive effort made toward the interpretation of silicon-29 chemical shifts in solution since the U curve was proposed in 1974. However, to clarify the implied role of the (d-p) π effect, we offer several observations.

Our interpretation of the U curve, in essence, amounts to the remark that the group electronegativity sum is not a particularly good measure of charge transfer when (d-p) π back-bonding is postulated. The type distinction reflects an effort to make consistent use of the group electronegativity concept, so that the sum might be a reasonable measure of charge transfer. Within this framework, the type P distinction is approximate, since ligands with both one and two available π -bonding orbitals per ligand are equated. The phenyl and vinyl electronegativities were chosen in accord with the original U curve data and are similar to values calculated elsewhere.³³

Variations in the silicon chemical shift are generally ascribed to changes in the paramagnetic shift contribution (σ^p), expressed in the Jameson-Gutowsky formalism:³⁴

$$\sigma^p = -\frac{2e^2\hbar^2}{3m^2c^2\Delta E}[\langle r^{-3} \rangle_p P_u + \langle r^{-3} \rangle_d D_u]$$

Typically the average excitation energy, ΔE , is assumed constant, and the shift is dependent on the bracketed sum. P_u and D_u reflect the charge density and asymmetry of the p and d electron clouds and are determined by σ and π effects, respectively (assuming orthogonality of the sp^3 - σ and d - π orbitals). The radial terms, $\langle r^{-3} \rangle_p$ and $\langle r^{-3} \rangle_d$, are determined by the effective nuclear charge and, consequently, depend on the nuclear screening induced by all the silicon valence electrons.

In 1968, Hunter and Reeves suggested that the qualitative features of the silicon chemical shifts were dominated by deshielding σ effects and shielding π effects.³⁵ One might infer that the observed shifts are a sum of deshielding $\langle r^{-3} \rangle_p P_u$ and shielding $\langle r^{-3} \rangle_d D_u$ terms and that the observed type P correlation is somehow a measure of total d occupancy. This is almost certainly not the case, based on the following reasoning. In silicates the Si-O nonbridging bond is almost always shorter than the Si-O-Si bridging bond. In the valence (d-p) π -bond formalism, this shortening is attributed to a higher nonbridging π -bond order.³⁶

The chemical shifts of the unpolymerized tetrahedra, which contain high (d-p) π -bond order, however, are greatly deshielded with respect to the polymerized tetrahedra. These observations are not in accord with a large shielding $\langle r^{-3} \rangle_d D_u$ term (which according to semiempirical calculations³⁷ may actually be small and deshielding). Moreover, the derived group fragment electronegativities are broadly as expected on the basis of σ -orbital electronegativities (allowing for crystal structure effects which seem to enhance the electronegativity of the larger cations).

Engelhardt, Radeglia, and co-workers (E&R) demonstrated that the U-curve inflection could originate from changes in $\langle r^{-3} \rangle_p P_u$ alone.³⁸ For increasing σ -bond ionicities, opposing deshielding $\langle r^{-3} \rangle_p$ and shielding P_u dependencies were noted (for electropositive silicon). We interpret our observations as consistent with a dominant $\langle r^{-3} \rangle_p P_u$ term, in which π effects may play an important role. For instance, according to Pauling's model for quartz, half the charge withdrawn by σ effects is back-donated through the π system so that the effective charge of silicon in quartz is equal to that of type S silicon of $\sum EN = 11.8$. Screening of the silicon nucleus due to π back-donation, however, is completely neglected in Slater's approximation used to evaluate $\langle r^{-3} \rangle_p$. According to SCF calculations, screening due to 3d interpenetration may be 86% as large as 3p screening.³⁹ The correlation observed between total σ and π contributions to the effective silicon charge and chemical shift may thus be due to changes in $\langle r^{-3} \rangle_p$. More generally, however, we expect that the charge transfer for type P species will be largely buffered by mesomeric π effects to satisfy electroneutrality. In the extreme instance where charge variation is completely buffered by mesomeric effects and screening is assumed independent of the valence orbital identity, then the $\langle r^{-3} \rangle_p$ term is constant and the type P correlation depends on P_u alone, which, in turn, is determined solely by σ effects. In the E&R model $\langle r^{-3} \rangle_p$ is weighted with an empirical factor generally less than one (although model dependent) for each ligand in a binding series (e.g., $Me_{4-n}SiCl_n$), to empirically account for imperfections in the Slater approximation (among other things). The empirical factor less than one effectively slows the increase of $\langle r^{-3} \rangle_p$ and may thereby mimic π effects neglected in the Slater approximation.

While these observations are necessarily tentative, they provide a plausible explanation for the influence of π effects on the chemical shift external to the $\langle r^{-3} \rangle_d D_u$ term. Thus π effects may shield the silicon nucleus by moderating changes in $\langle r^{-3} \rangle_p$ and may be accommodated in the E&R description of type M silicon by empirically weighting $\langle r^{-3} \rangle_p$.

Alternatively, Tossell has suggested that the chemical shifts in silicates are dominated by variations of ΔE , which he related to structural features using electronegativity-like arguments.¹³ Wolff and Radeglia have suggested that in organosilanes, ΔE , while not dominant, is charge dependent.⁴⁰ Our observations are not necessarily inconsistent with a dominant ΔE , although we believe that the corollary assumption that P_u is nearly constant in silicates requires further investigation.

Conclusions

The results we have presented above indicate that the use of group (fragment) electronegativities to predict silicon-29 shifts in silicates and aluminosilicates is a promising approach to the determination of the structures of these systems. The great advantages of the method is the ease and simplicity with which quite accurate chemical shift predictions can be made, from Q^0 to Q^4 sites in silicates, to aluminosilicates, and even to compounds containing linear SiOSi bonds (zunyite and petalite). On the basis of some 99 predicted chemical shifts (Table II), the mean absolute

(29) H. Effenberger, *Tsch. Min. Petr. Mitt.*, **27**, 129 (1980).

(30) L. Pauling, *Z. Kristallogr.*, **84**, 442 (1933).

(31) S. J. Louisnathan and G. V. Gibbs, *Am. Miner.*, **57**, 1089 (1972).

(32) A.-R. Grimmer, F. von Lampe, M. Tarmak, and E. Lippmaa, *Chem. Phys. Lett.*, **97**, 185 (1983).

(33) J. E. Huheey, *J. Phys. Chem.*, **70**, 2086 (1966). J. V. Bell, J. Heisler, H. Tannenbaum, and J. Goldenson, *J. Am. Chem. Soc.*, **76**, 5185 (1954).

(34) C. J. Jameson and H. S. Gutowsky, *J. Chem. Phys.*, **40**, 1714 (1964).

(35) B. K. Hunter and L. W. Reeves, *Can J. Chem.*, **46**, 1399 (1968).

(36) D. W. J. Cruickshank, *J. Chem. Soc. (London)*, 5486 (1961).

(37) R. Wolff and R. Radeglia, *Z. Phys. Chem. (Leipzig)*, **258**, 145 (1977).

(38) G. Engelhardt, R. Radeglia, H. Jancke, E. Lippmaa, and M. Magi, *Org. Magn. Reson.*, **5**, 561 (1973). R. Radeglia, *Z. Phys. Chem. (Leipzig)*, **256**, 453 (1975). R. Wolff and R. Radeglia, *Z. Phys. Chem. (Leipzig)*, **261**, 726 (1980).

(39) E. Clementi and D. L. Raimondi, *J. Chem. Phys.*, **38**, 2686 (1963).

(40) R. Wolff and R. Radeglia, *Org. Magn. Reson.*, **9**, 64 (1977).

deviation between experiment and prediction is 1.96 ppm, and the correlation coefficient between experiment and prediction of 0.979 is clearly better than the 0.88 value obtained with the bond energy-bond strength method,⁹ which until now has been the best predictor for ²⁹Si shifts when all types of sites (Q⁰-Q⁴) are considered.

- (41) K.-F. Hesse, *Acta Crystallogr., Sect. B*, **33**, 901 (1977).
 (42) W. S. McDonald and D. W. J. Cruickshank, *Acta Crystallogr.*, **22**, 37 (1967).
 (43) D. E. W. Vaughan, M. T. Melchior, and A. J. Jacobson, In "Intrazeolite Chemistry", G. D. Stucky and F. G. Dwyer, Eds., American Chemical Society, Washington, D.C., 1983, pp 231-242.
 (44) Y. Le Page, L. D. Calvert, and E. J. Gabe, *J. Phys. Chem. Solids*, **41**, 721 (1980).
 (45) W. A. Dollase, *Z. Kristallogr.*, **121**, 369 (1965).
 (46) G. V. Gibbs, C. T. Prewitt, and K. J. Baldwin, *Z. Kristallogr.*, **145**, 108 (1977).
 (47) H. Vollenkle, A. Wittmann, and H. Nowotny, *Monatsh. Chem.*, **100**, 295 (1969).

Acknowledgment. We thank R. J. Kirkpatrick for helpful discussions. This work was supported by the U.S. National Science Foundation Solid-State Chemistry Program (Grant DMR 8311339).

Registry No. ²⁹Si, 14304-87-1.

- (48) M. Kimata and N. Ii, *N. Jb. Miner. Mh.*, 1 (1981).
 (49) S. Saburi, I. Kusachi, C. Henmi, A. Kawahara, K. Henmi, and I. Kawada, *Miner. J.*, **8**, 240 (1976).
 (50) T. Yamanaka and H. Mori, *Acta Crystallogr., Sect. B*, **37**, 1010 (1981).
 (51) Y. Ohashi, *Phys. Chem. Miner.*, **10**, 217 (1984).
 (52) M. Cameron, S. Sueno, C. T. Prewitt, and J. J. Papike, *Am. Miner.*, **58**, 594 (1973).
 (53) C. T. Prewitt, *Z. Kristallogr.*, **125**, 298 (1967).
 (54) S. Sueno, M. Cameron, J. J. Papike, and C. T. Prewitt, *Am. Miner.*, **58**, 649 (1973).
 (55) V. F. Liebau, *Acta Crystallogr.*, **14**, 389 (1961).
 (56) B. Morosin, *Acta Crystallogr., Sect. B*, **28**, 1899 (1972).
 (57) R. H. Jarman, *J. Chem. Soc., Chem. Commun.*, 512 (1983).

Resonance Raman Spectra of O₂ Adducts of Cobalt Porphyrins. Enhancement of Solvent and Solute Bands via Resonance Vibrational Coupling

James R. Kincaid,* Leonard M. Proniewicz,[†] Krzysztof Bajdor,^{‡,§} Alan Bruha, and Kazuo Nakamoto*

Contribution from the Department of Chemistry, Marquette University, Milwaukee, Wisconsin 53233. Received February 26, 1985

Abstract: The resonance Raman spectra of O₂ adducts of cobalt porphyrin complexes with a large number of nitrogenous base axial ligands are reported. Evidence is presented for resonance enhancement of certain internal modes of the solvent (toluene or chlorobenzene) and, in some cases, internal modes of excess ligand molecules. The enhancement of these modes is shown to be dependent upon energy matching of the mode with the $\nu(\text{O}-\text{O})$ stretching frequency of the bound O₂. In addition, spectra of picket-fence porphyrin adducts indicate that such enhancement is critically dependent upon close association of the solvent or solute molecule with the bound O₂. These results are interpreted on the basis of resonance vibrational coupling resulting from an intermolecular interaction between bound O₂ and the solute or solvent molecule. Finally, a systematic study of the effect of axial ligand basicity on the frequency of $\nu(\text{O}-\text{O})$ yields a linear relationship between these two parameters over a range of basicities of more than nine orders of magnitude.

The potential of vibrational spectroscopy for the detection of subtle alterations in structure and bonding is well-recognized, and many investigators have applied infrared (IR) and resonance Raman (RR) spectroscopies to the study of oxygen binding to heme proteins and model compounds.¹⁻⁶ In fact, these techniques can provide a direct probe of the metal-oxygen linkage. Thus, the explicit goals of these types of studies are to identify the spectral features associated with the $\nu(\text{O}-\text{O})$, $\nu(\text{M}-\text{O})$, and $\delta(\text{M}-\text{O}-\text{O})$ modes and to precisely define the influence of steric, electronic, and environmental factors on the corresponding vibrational frequencies. Although a good deal of progress has been made recently, full realization of these goals has yet to be attained.

In principle, definitive assignment of the key modes can be made with the aid of isotopic labeling studies. However, correct interpretation of such data may be rendered difficult as a result of the inherent complexities of vibrational spectroscopy, such as vibrational coupling and Fermi resonance.⁷ For example, such

factors complicated the assignment of the $\nu(\text{O}-\text{O})$ in the IR spectra of oxyhemoglobin and model compounds wherein two isotope (¹⁶O₂/¹⁸O₂) sensitive bands were observed near 1100 and 1160 cm⁻¹.^{8,9} Subsequently, Alben and co-workers¹⁰ pointed out that

(1) Spiro, T. G. In "Iron Porphyrins"; Lever, A. P. B., Gray, H. B., Eds.; Addison-Wesley Publishing Co.: Reading, 1983; Part 11, p 89.

(2) Alben, J. O. In "The Porphyrins"; Dolphin, D., Ed.; Academic Press: New York, 1978; Vol. III, p 323.

(3) Asher, S. In "Methods in Enzymology"; Antonini, E., Rosi-Bernardi, L., Chiancome, E., Eds.; Academic Press: New York, 1981; Vol. 76, p 371.

(4) Friedman, J. M.; Rousseau, D. L.; Ondrias, M. R. *Annu. Rev. Phys. Chem.* **1982**, **33**, 471.

(5) Kitagawa, T.; Ondrias, M. R.; Rousseau, D. L.; Ikeda-Saito, M.; Yonetani, T., *Nature (London)* **1982**, **298**, 869.

(6) Felton, R. H.; Yu, N.-T. In "The Porphyrins"; Dolphin, D., Ed.; Academic Press: New York, 1978; Vol. III, p 367.

(7) Wilson, E. B., Jr.; Decius, J. C.; Cross, P. C. "Molecular Vibrations"; McGraw-Hill: New York, 1955.

(8) (a) Barlow, C. H.; Maxwell, J. C.; Wallace, W. J.; Caughey, W. S. *Biochem. Biophys. Res. Commun.* **1973**, **55**, 91. (b) Maxwell, J. C.; Volpe, J. A.; Barlow, C. H.; Caughey, W. S. *Biochem. Biophys. Res. Commun.* **1974**, **58**, 166.

(9) Collman, J. P.; Brauman, J. I.; Halbert, T. R.; Suslick, K. S. *Proc. Natl. Acad. Sci. U.S.A.* **1976**, **73**, 3333.

* Permanent address: Regional Laboratory of Physicochemical Analyses and Structural Research, Jagiellonian University, Cracow, Poland.

[†] Permanent address: Technical University of Wroclaw, Wroclaw, Poland.

[§] Present address: Department of Chemistry, University of Oregon, Eugene, OR.